Proc. Indian Acad. Sci. (Earth Planet. Sci.), Vol. 105, No. 3, September 1996, pp. 309–323.

An analysis of MONTBLEX data on heat and momentum flux at Jodhpur

KUSUMA G RAO, R NARASIMHA and A PRABHU†

Jawaharlal Nehru Centre for Advanced Scientific Research, Bangalore 560094, India
†Centre for Atmospheric Sciences, Indian Institute of Science, Bangalore 560012, India

Abstract. Parameterization of sensible heat and momentum fluxes as inferred from an analysis of tower observations archived during MONTBLEX-90 at Jodhpur is proposed, both in terms of standard exchange coefficients C_H and C_D respectively and also according to free convection scaling. Both coefficients increase rapidly at low winds (the latter more strongly) and with increasing instability. All the sensible heat flux data at Jodhpur (wind speed at 10 m $\bar{U}_{10} < 8\,\mathrm{ms}^{-1}$) also obey free convection scaling, with the flux proportional to the '4/3' power of an appropriate temperature difference such as that between 1 and 30 m. Furthermore, for $\bar{U}_{10} < 4\,\mathrm{ms}^{-1}$ the momentum flux displays a linear dependence on wind speed.

Keywords. Sensible heat flux; momentum flux; free convection; exchange coefficient of heat; drag coefficient.

1. Introduction

It has been shown by Beljaars and Miller (1990) and Miller *et al* (1992) that the model in use at the European Centre for Medium Range Weather Forecasting produces a more realistic climatological rainfall pattern over India with an improved parameterization for evaporation and sensible heat flux at low winds over the oceans. The improvement seeks to account for an enhancement of the fluxes because of the 'gustiness' due to dry convective motion near the surface, and provides modified transfer coefficients for heat and moisture flux at low winds that are in accord with a scaling law for free convection. At a time when flux data at low winds over the oceans were scarce, the rationale for the modified parameterization adopted by Miller *et al* (1992) was that the evaporation from the ocean cannot be smaller than that from an aerodynamically smooth water surface, i.e., that free convection provided a reliable lower bound. This argument goes back to Deardorff (1972), who recommended that the sensible heat flux in the convective boundary layer should be constrained to be no smaller than that associated with free convection. Following the arguments of Townsend (1964) the heat flux then takes the form

$$Q_s = (\overline{w'\theta'})_s = C_s \left(\frac{g}{\theta_m} \frac{\kappa^2}{\nu} \right)^{1/3} (\theta_s - \theta_m)^{4/3}, \tag{1}$$

where κ is the molecular thermal diffusivity, ν is the kinematic viscosity, θ_s is the surface temperature, θ_m is the (constant) potential temperature within the mixed layer, g is the acceleration due to gravity and Q_s represents the surface value of the eddy sensible heat

flux $\overline{w'\theta'}$. C_s is a constant whose value was given as 0·20 by Townsend, and as in the range 0·1 to 0·24 by Deardorff and Willis (1985).

The free convection limit has a long history (Prandtl 1932; Priestley 1954). In the corresponding limit of Monin-Obukhov theory, the non-dimensional temperature gradient should approach $(-\zeta)^{-1/3}$ at large negative $\zeta \equiv z/L$ where z is height above ground and L represents the Monin-Obukhov length. That is

$$\phi_\theta \equiv \frac{k}{\theta_*}\frac{\partial\theta}{\partial \log z} \sim (-\zeta)^{-1/3} \quad \text{as} \quad -\zeta \to \infty, \tag{2}$$

where k represents the von Karman constant ($\sim 0{\cdot}4$) and θ_* the friction temperature. However Businger *et al* (1971) and Businger (1988), using the well-known Kansas observations, conclude that the non-dimensional temperature gradient approaches $(-\zeta)^{-1/2}$ at large negative ζ. A critical analysis of these two proposals is presented by Tennekes (1973). A different perspective is provided by Schumann (1988), who postulates a simple model for the surface layer of a convective boundary layer at zero mean wind over a homogeneous rough surface. This model suggests that the temperature difference between the ground and the mixed layer increases with the ratio of boundary layer height to roughness length. Schumann concludes that the appropriate heat transfer relationship in terms of Nusselt and Rayleigh numbers is $\mathrm{Nu} \sim \mathrm{Ra}^{1/2}$ in the rough case (in agreement with the form proposed by Businger), and argues that the relationship $\mathrm{Nu} \sim \mathrm{Ra}^{1/3}$ (corresponding to (1)) is valid for smooth surfaces at Rayleigh numbers less than a critical value that depends on the ratio of boundary layer thickness to roughness height.

Beljaars and Miller (1990) and Miller *et al* (1992) finally use modified exchange coefficients in the bulk aerodynamic formulae to estimate heat and moisture fluxes. Bulk aerodynamic parameterization of the fluxes is perhaps the most commonly used approach in operational boundary layer and general circulation models. Nevertheless the question of the correct parameterization of fluxes under highly unstable conditions continues to be of great current interest (Beljaars 1994; Stull 1994), and cannot yet be considered to have been satisfactorily resolved.

Most of the observational evidence with regard to heat flux has till recently come from the oceans. Thus Large and Pond (1982) suggest that

$$\begin{aligned} 10^3 C_H &= 1{\cdot}13, \quad z/L < 0, \quad 4 < \bar{U}_{10} < 25\,\mathrm{ms}^{-1}, \\ &= 0{\cdot}66, \quad z/L > 0, \quad 6 < \bar{U}_{10} < 20\,\mathrm{ms}^{-1}, \end{aligned} \tag{3}$$

using the temperature differential between sea-surface and 10 m as reference. At low winds there is only the study of Bradley *et al* (1991) over the Pacific warm pool region. There have been very few studies over land and none over the monsoon region.

The main aim of the present paper is to propose a parameterization for the sensible heat flux in terms of temperature differentials between the ground and the air above, as inferred from an analysis of observations archived during the Monsoon Trough Boundary Layer Experiment, 1990 (Goel and Srivastava 1990; Sikka and Narasimha 1995). We report results using both the standard exchange coefficient as it depends on wind speed, stability and roughness, especially at low winds, and also free-convection scaling, along the lines of Townsend (1964) and Schumann (1988).

The results on the exchange coefficient are presented in § 3 and the free convection scaling in § 4. A brief comment on the momentum fluxes at low winds, in the light of the present conclusions on heat flux, is made in § 5.

2. Data analysed

Results are analysed for one station, namely Jodhpur (26·3N, 73E), using micrometeorological tower observations (Rudra Kumar *et al* 1995). The period chosen for analysis extends from 9th June to 20th August covering almost the entire duration of the experiment. Measurements were made by cup and sonic anemometers and platinum wire resistance thermometers mounted on a 30 m tower. The sonic anemometer was placed at 4 m above the surface, the cup anemometers at six heights namely 1, 2, 4, 8, 15 and 30 m, and the thermometers at four heights namely 1, 8, 15 and 30 m.

High frequency (8 Hz) observations of turbulence and the virtual temperature were obtained from the sonic anemometer. The data are available at hourly intervals during intensive observation periods (Srivastav 1995), otherwise at three-hourly intervals continuously for 10 min (15 min) from 15th June to 7th July (June 6th–14th; July 8th–August 20th). The total number of observations available is 676. Details about the tower site and estimates of the roughness length at site are available in Kusuma (1995). Rudra Kumar *et al* (1995) discuss the instrumentation, the accuracy of the measurements, and the quality control procedures adopted.

The methods used for computing momentum and heat fluxes, the friction velocity u_* and the drag coefficient C_D are described in Kusuma *et al* (1995). The friction temperature θ_* is obtained here as

$$\theta_* = \frac{-\overline{w'\theta'}}{u_*}, \tag{4}$$

and the exchange coefficient for heat (using the velocity $\bar{U}_{10}$ at 10 m as reference) as

$$C_H = \frac{+\overline{w'\theta'}}{\bar{U}_{10}\Delta\theta}, \tag{5}$$

where $\bar{U}_{10}$ is obtained by fitting a least-square quadratic curve to the observed velocities along the mean wind direction at six heights and $\Delta\theta$ is an appropriate temperature differential.

A good candidate for $\Delta\theta$ would appear to be the difference $\theta_g - \theta_{10}$, where θ_{10} can be obtained by curve-fitting to measured temperatures at four heights. As the ground temperature θ_g was unfortunately not measured, we use the values given by Rao (1995) as calculated by solving a heat conduction equation using sub-soil temperatures. A comparison of observed ground temperatures (at a different site) with those estimated by this procedure reveals generally good agreement but differences occasionally as large at 5°C or even more. In general, the use of ground temperatures for defining heat exchange coefficients presents certain problems. Whereas over the oceans the use of the sea-surface temperature is convenient (because of approximate horizontal homogeneity), ground temperature can vary widely and rapidly over land. We shall

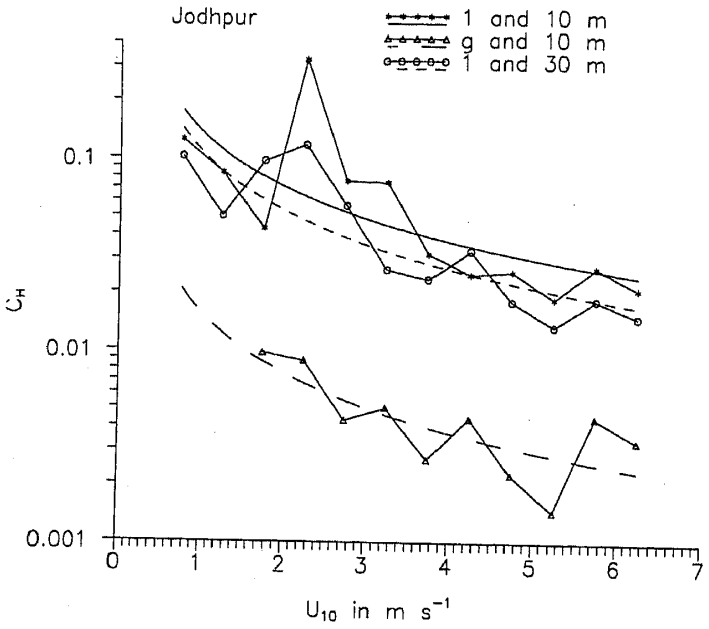

Figure 1. Variation of exchange coefficient of heat, C_H with wind speed for $\Delta\theta = T_g - T_{10}$, $T_1 - T_{10}$ and $T_1 - T_{30}$.

Table 1. Mean and standard deviation (std) of C_H.

N	*DT*	Mean C_H	Std C_H
1	T_1–T_{10}	0·083	0·037
2	T_1–T_{30}	0·048	0·009
3	T_g–T_{10}	0·005	0·001

argue here that for this reason other temperature differentials may be more appropriate in parameterizing heat flux, whether through (1) or (5).

3. Exchange coefficient

3.1 *Dependence on wind speed*

The exchange coefficient for heat, C_H, estimated according to formula (5), is presented in figure 1 as a function of wind speed for three combinations of temperature differentials: $T_g - T_{10}$, $T_1 - T_{10}$ and $T_1 - T_{30}$, where the subscript denotes height in metres, T_1 and T_{30} are observed temperatures and T_{10} is obtained by fitting a least square quadratic curve to the observed temperatures. Each point in figure 1 is an average over a velocity bin of 0·5 m s^{-1}. All the results presented are for the period 9th June to 2nd July: the data from 3rd July to 20th August present certain difficulties that will be

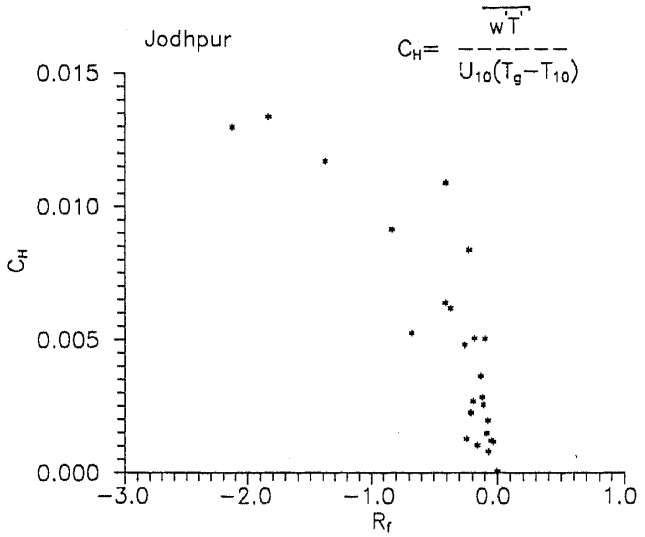

Figure 2. Variation of exchange coefficient of heat, C_H (with $\Delta\theta = T_g - T_{10}$) with flux Richardson number, R_f.

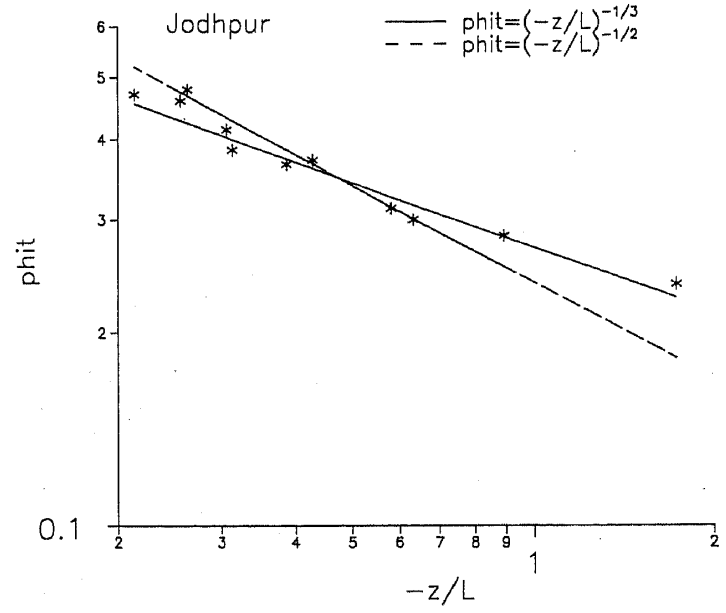

Figure 3. Variation of non-dimensional temperature gradient, ϕ_θ with $-\zeta = -z/L$.

discussed later. A strong dependence of C_H on wind speed is revealed in all the three estimations of C_H in figure 1. However, the absolute values of C_H obtained here cannot be compared directly with other studies as the temperature differentials used here are not the same. The mean and standard deviation (std) for all three estimations of C_H, shown in table 1, suggests that the scatter is much less if the temperature difference between the ground and the 10 m level is chosen as reference. It is interesting that the dependence of C_H on wind speed at low winds is weaker than that of the drag coefficient, as we shall discuss in § 5.

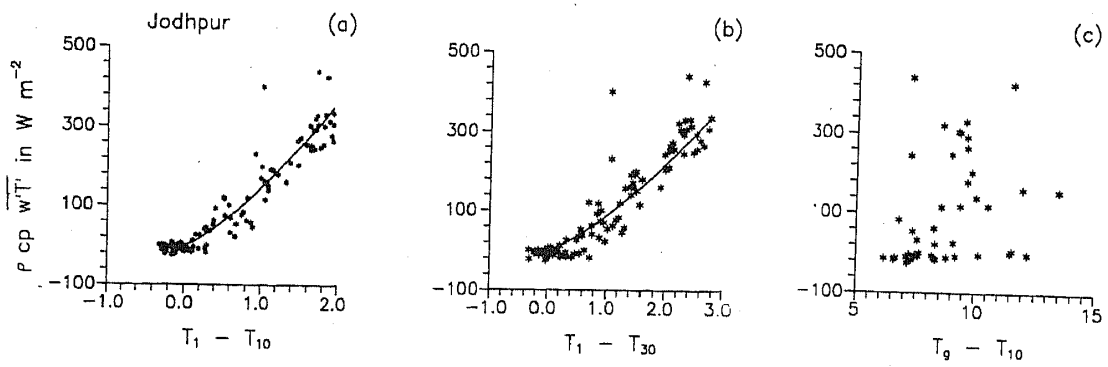

Figure 4. Sensible heat flux (Wm^{-2}) variation with DT taken as (**a**) $T_1 - T_{10}$, (**b**) $T_1 - T_{30}$, (**c**) $T_9 - T_{10}$.

Although in certain models a prescription of C_H on wind speed may be of use, such a relation is not satisfactory (if only for dimensional reasons), and we explore below other methods of analysis of the flux data that may lend themselves to better extrapolation to other situations.

3.2 *Dependence on stability*

We analyse here the effect of stability through the flux Richardson number, defined as

$$R_f = (g/\bar{\theta}) \frac{\overline{w'T'}}{\overline{U'w'}(\partial \bar{U}/\partial z)},$$

where U' is the velocity fluctuation along the mean wind direction. Figure 2 shows the dependence of C_H on R_f for the temperature differential between the ground and 10 m. In agreement with earlier studies (Stull 1988), the coefficient increases with increasing instability. The large values of C_H under strongly unstable conditions at low winds suggest free convection, which we study in the next section.

The same tendency is seen even if C_H is calculated with other temperature differentials, namely between 1 and 10 m and between 1 and 30 m.

4. Free convection scaling

4.1 *Non-dimensional temperature gradient*

The variation of daytime (0700 to 1800IST) sensible heat flux and friction velocity as a function of wind speed, for the period from 9th June to 20th August (figures not shown), suggests that both quantities are significant at low winds, the heat flux going up to values of 300 Wm^{-2} and u_* varying between 0·12 and 0·36 ms^{-1} for winds < 2 ms^{-1}; u_* increases with wind speed as expected. These large values at low winds suggest that associated convective motions could be the cause. To study this question we construct the non-dimensional temperature gradient according to equation (2) and plot ϕ_θ (labelled phit) versus $-\zeta$ in figure 3. (The temperature gradient is determined by curve

fits to the recorded temperatures, and is evaluated at a height of 4 m). Both the Prandtl and Businger-Dyer limits are shown on the diagram for comparison. It is seen that while a $(-\zeta)^{-1/2}$ law may be valid for $-\zeta < \sim 0{\cdot}6$, the values at $-\zeta \sim 1$ to 2 are more consistent with a $(-\zeta)^{-1/3}$ law, valid over almost the whole range $-\zeta > 0{\cdot}2$. It would appear that the condition for the validity of free-convection scaling is much weaker than that quoted by Monin and Yaglom (1975), namely that $-\zeta \gg 1$.

4.2 *Sensible heat flux*

A plot of heat flux versus the temperature difference between 1 and 10 m is shown in figure 4(a). The solid line here, as represented by

$$Q_s = 145(DT)^{4/3}, \tag{6}$$

where $DT = T_1 - T_{10}$, is the best fit to the Townsend '4/3' power law variation (1). The constant C_s in equation (1) as evaluated with the present data turns out to be 12·3, with an average temperature difference of 1·1°C as given in table 2. Figure 4(b) shows that the heat flux approaches $(DT)^{4/3}$ even when $DT = T_1 - T_{30}$, but with a different constant equal to 85 in (6), and $C_s = 7{\cdot}2$ in (1), for an average temperature difference of $DT = 1{\cdot}5$°C (table 2). When we use the temperature difference between the ground and 10 m the scatter is too large (figure 4c).

4.3 *Dependence on roughness*

The roughness length at Jodhpur varies with the sector in which the wind is blowing; in the 'smooth' or open sector (between 200° and 230°) where the terrain is relatively flat and obstacle-free, it is 1·2 cm; and in the sector outside 200° and 230° it is highly variable, with an average value of 6·8 cm. We will call this the 'rough' sector, although it is actually not homogeneous (Kusuma 1995). Plots similar to figure 4 for the heat flux with $DT = T_1 - T_{10}$ are shown in figure 5(a and b) for the smooth and rough sectors separately. Comparing with figure 4(a), we find that figure 5(a) shows much less scatter in the smooth sector; and figure 5(b) shows that the outliers of figure 4(a) are from the rough sector. However figure 5(a and b) depicts the 4/3 power variation irrespective of sector, revealing that the overall variation is independent of roughness. The corresponding C_s values for the smooth and the rough sectors are 11·3 and 13·4 (see table 2).

According to Schumann (1988), the heat flux follows the relation $\mathrm{Nu} \sim \mathrm{Ra}^{1/3}$ for a smooth surface and $\mathrm{Nu} \sim \mathrm{Ra}^{1/2}$ for a rough surface; the former is valid for all Rayleigh numbers less than a critical value that depends on the ratio of boundary layer height to

Table 2. C_s values.

N	Levels	DT(°C)	$Q_s/(DT)^{4/3}$	C_s	Sector
1	1 and 10 m	1·1	144·7	12·28	Entire.
2	1 and 30 m	1·5	85·0	7·22	Entire.
3	1 and 10 m	1·1	133·3	11·3	Smooth.
4	1 and 10 m	1·1	158·0	13·4	Rough.
5	1 and 30 m	1·6	87·8	7·5	Smooth.
6	1 and 30 m	1·5	115·2	9·8	Rough.

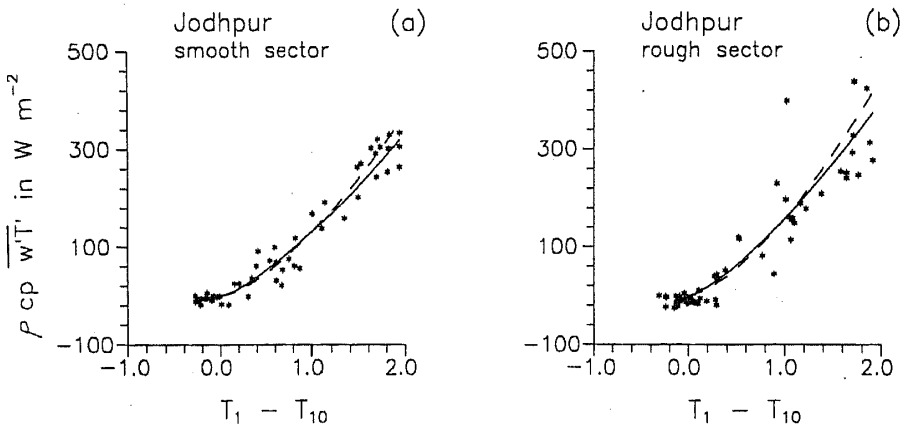

Figure 5. Sensible heat flux (Wm^{-2}) variation with $DT = T_1 - T_{10}$ for (**a**) smooth sector, (**b**) rough sector. Dashed line represents '3/2' fit and solid line represents '4/3' fit.

roughness length. Because we do not know the boundary layer height from the present data, a '3/2' power fit (corresponding to the relation for a rough surface) was also made to the data in figure 5(a and b) and is shown by dashed lines. Not surprisingly, the differences between the two fits are not significant.

However, if we assume the boundary layer height h as 1(2)km, the critical Rayleigh number according to Schumann (1988),

$$\mathrm{Ra} = 560(h/20)^{8/3},$$

takes the value of $6{\cdot}9 \times 10^{15}(4{\cdot}4 \times 10^{16})$ for $\mathrm{Pr} = 0{\cdot}7$, $(z_0 u_*)/\nu > 10$, where Pr is the Prandtl number. Estimates of the Rayleigh number

$$\mathrm{Ra} = \frac{(g/T)h^3 \Delta\theta}{\kappa\nu}$$

for the present observations may be made using $\Delta\theta = T_1 - T_{10}$, which is usually appreciably less than the differential $\Delta\theta = \theta_g - \theta_m$ used by Schumann. Nevertheless, it turns out that the values of Ra estimated here are larger than the Schumann critical Rayleigh number by two to three orders magnitude. Thus, according to Schumann, the heat flux should obey a '3/2' rather than a '4/3' power law. However we do not see any significant difference between fits assuming either law for the range of temperature differences observed here (which, at $< 2°$, are small compared to the example quoted by Schumann of 9·8 K between θ at roughness height and in the mixed layer). Differences between the two fits will also be larger only if the temperature differences are larger. The value of $z_0 u_*/\nu \sim 160$ suggests that the present data correspond to a convective boundary layer over a rough surface though z_0 is quite small (at 1·2 cm). Thus there is no evidence here to support the dependence of the heat flux relationship on the ratio h/z_0 in the present case. However Schumann's criterion on critical Rayleigh number cannot be subjected to a serious test by the present data as we do not know the boundary layer height or the temperatures at roughness height and in the mixed layer. Nevertheless it is established beyond doubt from the present analysis that the observed

heat flux scales very well according to free convection theory for temperature differentials between 1 and 10 m as well as between 1 and 30 m.

In table 3, the root mean square (rms) deviations of the heat flux from '4/3' and '3/2' laws are presented for both temperature differentials in the two sectors. It is seen that the deviations are smaller for $DT = T_1 - T_{10}$ than for $T_1 - T_{30}$; however we see contrasting differences between the smooth and rough sectors. There is no significant difference in the rms deviations of the heat flux between the two fits.

All the results presented in § 4 are for the period from 9th June to 2nd July. The data between 3rd July and 20th August appear to have been subject to an undocumented change in calibration: the reason for this suspicion is that during this period DT is never negative (as we may expect it to be at least during night), and that in a plot of Q_s vs. DT the best-fit curve is shifted to the right by about 1·5° compared to that in figure 4. A correction by this amount produces excellent agreement between the two data sets, but we have not ventured to present it in the absence of other more direct evidence and calibration data during the period.

5. Momentum flux

The dependence of the drag coefficient on wind speed has been analysed by Mohanty *et al* (1995) and Kusuma *et al* (1996) using somewhat different approaches. The latter work discusses the effect of stability and roughness in detail, so we confine ourselves here to a discussion of the momentum flux in the free-convection regime.

5.1 *Drag coefficient*

Figure 6 shows a comparison of the dependence of C_D and C_H (with $\Delta\theta = T_g - T_{10}$ on wind speed. The rapid increase of both C_D and C_H at low winds (although at different rates) suggests a need for a drag parameterization that is consistent with the heat flux parameterization of § 4 for application in large-scale models.

Figure 7(a), which shows the drag variation with wind speed for $R_f < 0{\cdot}03$, suggests that drag is not only significant at low winds but varies nearly linearly with wind speed, i.e., the drag coefficient increases approximately like $\bar{U}_{10}^{-1}$. However, low winds are not characterized exclusively by a flux Richardson number that takes large negative values, i.e., by strongly unstable situations associated with free convection; there are also

Table 3. Root mean square values.

N	Levels	RMS values for '4/3' law (Wm^{-2})	RMS values for '3/2' law (Wm^{-2})	Sector
1	1 and 10 m	48·0	52·5	Entire.
2	1 and 30 m	51·9	52·3	Entire.
3	1 and 10 m	32·5	35·1	Smooth.
4	1 and 10 m	57·0	62·6	Rough.
5	1 and 30 m	34·3	44·0	Smooth.
6	1 and 30 m	67·1	83·2	Rough.

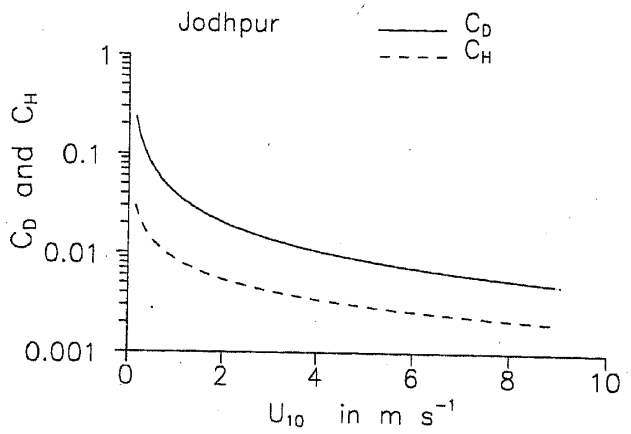

Figure 6. Comparison between drag coefficient, C_D and exchange coefficient of heat, C_H as a function of wind speed.

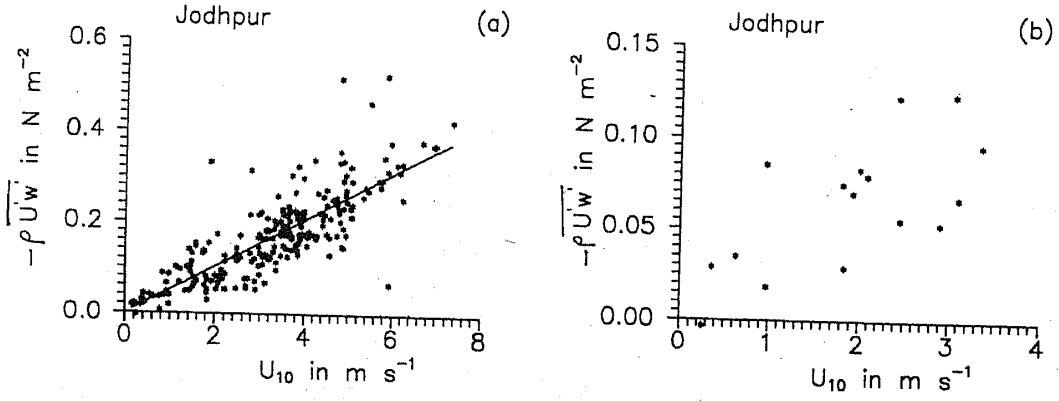

Figure 7. The variation of drag in Nm^{-2} with wind speed for (**a**) $R_f < 0{\cdot}03$, (**b**) strong unstable conditions ($-4{\cdot}0 < R_f < -1{\cdot}0$).

situations when conditions can be nearly neutral. If we select data points only for strongly unstable conditions ($-4{\cdot}0 < R_f < -1{\cdot}0$), we obtain figure 7(b). It is seen that the data are again consistent with an approximate inverse dependence of C_D on $\bar{U}_{10}$ at low winds, although the number of data points is too small to draw a firm conclusion. We may speculate that, as drag must vanish in true windless free convection, its dependence on wind speed at low winds must be linear. That the same kind of variation holds under near-neutral conditions also suggests that low-wind parameterizations may be more complex than hitherto considered. This must remain a subject for further study.

5.2 *Non-dimensional wind shear*

The non-dimensional wind shear, $\phi_m = (\kappa z/u_*)\partial\bar{u}/\partial z$, is calculated at two heights, namely 4 m (where the sonic measurements are made) and 30 m. The shear $\partial\bar{u}/\partial z$ is obtained by fitting a least-square curve to cup winds at all six heights, and u_* is estimated from sonic measurements. A comparison of the non-dimensional shear

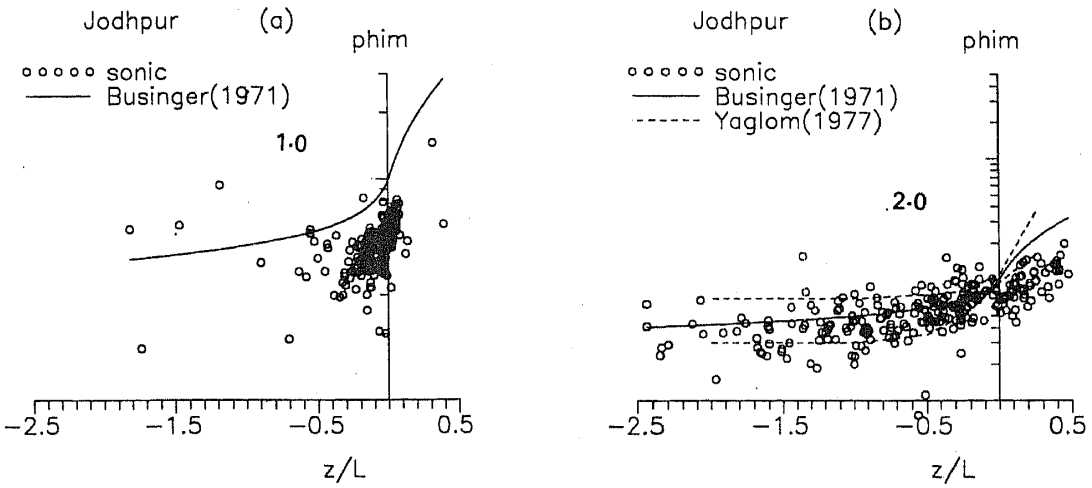

Figure 8. A comparison of non-dimensional wind shear, ϕ_m observed with Businger's expression at (**a**) 4 m, (**b**) 30 m.

inferred from the present data with that proposed by Businger *et al* (1971) is presented in figure 8(a and b). The agreement with Businger's curve is not perfect, but the scatter seen here at 30 m is well within the range of ϕ_m recommended by various authors in the near-neutral and unstable regimes, as compiled by Yaglom (1977).

6. Monin-Obukhov similarity

Since exchange coefficients in many general circulation models are based on the Monin-Obukhov theory and Businger *et al*'s (1971) flux-profile relations, we present here a comparison between the values of u_* and θ_* thus estimated with the observed values.

It is seen from figure 9(a–f) that at high winds there is good agreement whereas at low winds and unstable conditions there is substantial disagreement; even under neutral conditions the observed u_* is higher at low winds. (The latter data supplement those in Kusuma G Rao *et al* 1996.)

The flux-profile calculations shown in figure 9 are based on data at roughness height and 10 m level. Further calculations made here suggest that similar conclusions follow even if we choose any level other than 10 m, but that the agreement is poor if the roughness height is not one of the levels. All these results suggest that a careful re-examination of the Monin-Obukhov theory under low wind/free convection conditions is now required, as also recently suggested by Beljaars (1994).

7. Conclusions

In the light of the analysis made here of heat and momentum flux data acquired at Jodhpur during MONTBLEX, it is concluded that if the fluxes are parameterized by bulk aerodynamic formulae, it is necessary to take dependence on wind speed into

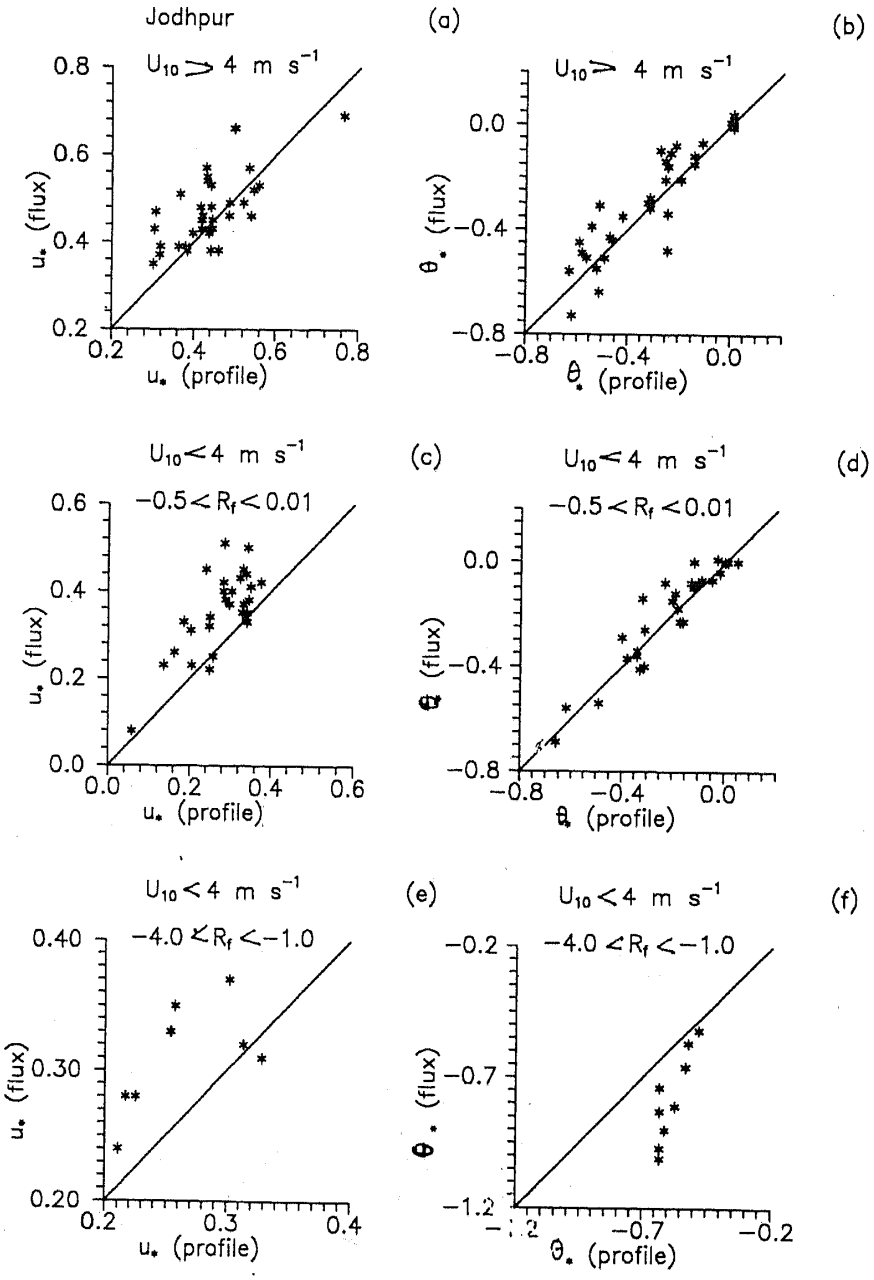

Figure 9. Comparison of u_* and θ_* at Jodhpur obtained by profile and eddy correlation methods: **(a, b)** for $\bar{U}_{10} > 4\,\mathrm{ms}^{-1}$ and the entire range of stability; **(c, d)** for $\bar{U}_{10} < 4\,\mathrm{ms}^{-1}$ and near neutral stability; **(e, f)** for $\bar{U}_{10} < 4\,\mathrm{ms}^{-1}$ and strongly unstable conditions.

account. At Jodhpur the drag data can be represented approximately by the formula

$$C_D = 0{\cdot}04\,\bar{U}_{10}^{-1}, \quad \bar{U}_{10} < 4\,\mathrm{ms}^{-1}.$$

We are unable to confirm this dependence at Kharagpur as wind speeds there rarely fell below $3\,\mathrm{ms}^{-1}$. This parameterization is unsatisfactory if only because it is dimensional. At the present stage both further analysis and observational data are required to arrive at a more satisfactory parameterization. As the above formula suggests that drag

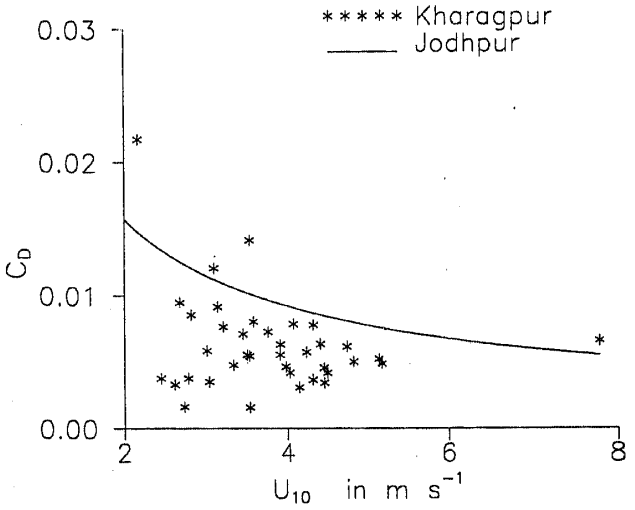

Figure 10. Comparison of drag coefficient between Kharagpur and Jodhpur for the smooth sector.

increases *linearly* with wind speed at low winds, one is tempted to attribute the finding to the dominance of free convection, but this conclusion is not supported by the fact that the linear dependence on velocity seems to characterize the data at nearly neutral conditions as well. (It must be noted that low winds can occur in all stability regimes: highly unstable nearly windless free convection, neutrally stable conditions during daytime associated with rain or cloudiness and also during the transitional epochs (morning and evening), and stable nocturnal conditions). Furthermore, at wind speeds $> 3\,\mathrm{ms}^{-1}$, C_D at Kharagpur is about half that at Jodhpur even in the smooth sector (figure 10), although the roughness heights are comparable (1·2 and 1·9 cm). The evidence therefore suggests that all the variables that are necessary to formulate satisfactory parameterization schemes have not yet been identified.

This conclusion is also supported by the heat flux measurements. However the difference here is that the heat flux is well described by free convection scaling. Indeed we recommend that the sensible heat flux be taken as

$$Q_s = C_s \left(\frac{gK^2}{\theta\, \nu}\right)^{1/3} (DT)^{4/3},$$

where DT represents a characteristic temperature differential. We suggest that a convenient measure of DT is the difference in temperature between 1 m and 30 m; for this choice the constant C_s takes the value 7·5 in the smooth sector at Jodhpur (roughness length = 1·2 cm). There is evidence that the constant C_s above varies with roughness, increasing slightly to 9·8 in the rough sector (average roughness length 6·8 cm). While the free convection 4/3 power law is recommended, the reason for this is chiefly that the argument for the scaling is both plausible and attractive, and is in good accord with observations. However, a 3/2 power law, which would be consistent with the Businger stability functions, would also perform reasonably well. At the same time estimates of u_* and θ_* using the Businger flux-profile relationships do not agree well with observed values at low winds thus raising questions about the applicability of the Monin-Obukhov theory to conditions actually prevailing in the atmospheric boundary layer.

In spite of the theoretical questions that still need to be tackled, it is believed that the present analysis shows how the parameterization of both momentum and heat flux can be made more realistic for use in large-scale circulation models.

Acknowledgements

This work was carried out as part of a project supported by the Department of Science and Technology, Government of India.

References

Beljaars A C M 1994 The parameterization of surface flux in large scale models under free convection; *Q. J. R. Meteorol. Soc.* **121** 255–270

Beljaars A C M and Miller M J 1990 The sensitivity of the ECMWF model to the parameterization of evaporation from the tropical oceans; *ECMWF technical memorandum* no 170

Bradley E F, Coppin P A and Godfrey J S 1991 Measurements of sensible and latent heat flux in the western equatorial Pacific Ocean; *J. Geophys. Res. (Suppl.)* **96** 3375–3389

Businger J A 1988 A note on the Businger-Dyer profiles; *Boundary-Layer Meteorol.* **42** 145–151

Businger J A, Wyngaard J C, Izumi Y and Bradley E F 1971 Flux-profile relationship in the atmospheric surface layer; *J. Atmos. Sci.* **28** 181–189

Deardorff J W 1972 Parameterization of the planetary boundary layer for use in general circulation models; *Mon. Weather Rev.* **2** 93–106

Deardorff J W and Willis G E 1985 Further results from a laboratory model of the convective planetary boundary layer; *Boundary-Layer Meteorol.* **32** 205–236

Goel M and Srivastava H N 1990 Monsoon Trough Boundary Layer Experiment (MONTBLEX); *Bull. Am. Meteorol. Soc.* **71** 1594–1600

Kusuma G Rao 1996 Roughness length and drag coefficient at two MONTBLEX-90 tower stations; *Proc. Indian Acad. Sci. (Earth Planet. Sci.)* **105** 273–287

Kusuma G Rao, Narasimha R and Prabhu A 1996 Estimation of drag coefficient at low wind speeds over the monsoon trough land region during MONTBLEX-90; *Geophys. Res. Lett.* (in press)

Kusuma G Rao, Sethu Raman, Prabhu A and Narasimha R 1995 Surface turbulent heat flux variation over the monsoon trough region during MONTBLEX-90; *Atmos. Environ.* **29** 2113–2129

Large W G and Pond S 1982 Sensible and latent heat flux measurements over the ocean; *J. Phys. Oceanogr.* **12** 464–482

Miller M J, Beljaars A C M and Palmer T N 1992 The sensitivity of the ECMWF model to the parameterization of evaporation from the tropical oceans; *J. Climate* **5** 418–434

Mohanty U C, Parihar P S, Venugopal T and Parashuram 1995 Estimation of the drag coefficient over the western desert sector of the Indian summer monsoon trough; **104** 273–287

Monin A S and Yaglom A M 1975 *Statistical hydrodynamics.* (Cambridge, MA: MIT Press)

Prandtl L 1932 Meteorologische Anwendung der stromungslehre; *Beitr Phys. für Atmosph.* **19** 188–202

Priestley C H B 1954 Convection from a large horizontal surface; *Australian J. Phys.* **7** 176–201

Rao K Narahari 1995 Estimation of surface temperature from MONTBLEX-data; *Proc. Indian Acad. Sci. (Earth Planet. Sci.)* **104** 257–271

Rudra Kumar S, Ameenulla S and Prabhu A 1995 MONTBLEX tower observation: Instrumentation, data acquisition and data quality; *Proc. Indian Acad. Sci. (Earth Planet. Sci.)* **104** 221–248

Schumann U 1988 Minimum friction velocity and heat transfer in the rough surface layer of a convective boundary layer; *Boundary-Layer Meteorology* **44** 311–326

Sikka D R and Narasimha R 1995 Genesis of the monsoon trough boundary layer experiment (MONTBLEX); *Proc. Indian Acad. Sci. (Earth Planet. Sci.)* **104** 157–187

Srivastav S K 1995 Synoptic meteorological observations and weather conditions during MONTBLEX-90; *Proc. Indian Acad. Sci. (Earth Planet. Sci.)* **104** 189–220

Stull R B 1988 An introduction to boundary layer meteorology (Dordrecht, The Netherlands: Kluwer Academic Publishers)

Stull R B 1994 A convective transport theory for surface fluxes; *J. Atmos. Sci.* **51** 3–22

Tennekes H 1973 Similarity laws and scale relations in planetary boundary layers. In: *Workshop on micrometeorology* (ed.) D A Hangen (American Met. Soc.) 177–216

Townsend A A 1964 Natural convection on water over an ice surface; *Q. J. R. Meteorol. Soc.* **90** 248–259

Yaglom A M 1977 Comments on wind and temperature flux-profile relationship; *Boundary-Layer Meteorol.* **11** 89–102